

## Structural characterization of some borate glass specimen by ultrasonic, spectroscopic and SEM studies

S Thirumaran<sup>1\*</sup> & N Prakash<sup>2</sup>

<sup>1</sup>Department of Physics (DDE), Annamalai University, Annamalai Nagar 608 002, India

<sup>2</sup>Department of Physics, Annamalai University, Annamalai Nagar 608 002, India

\*E-mail: thirumaran64@gmail.com

Received 17 March 2014; revised 24 December 2014; accepted 8 January 2015

The ultrasonic wave velocity (longitudinal and shear) and density for the ternary glass system of (i)  $B_2O_3-SiO_2-Na_2CO_3$  (BSS-glass systems) and (ii)  $B_2O_3-Bi_2O_3-Na_2CO_3$  (BBS-glass systems) have been measured at room temperature by using pulse-echo technique at 5MHz. The glass samples were prepared by conventional melt-quenching method. The amorphous nature of the glass samples was ascertained using X-ray diffractometry (XRD). The measured experimental values have been utilized to evaluate the elastic moduli, Poisson's ratio, acoustic impedance, micro hardness, Debye temperature, thermal expansion coefficient and oxygen packing density which are discussed in terms of the structural changes in the glass specimen. The functional groups present in the glass samples have been confirmed by FTIR spectral analysis. The surface morphology of the glass samples has also been thoroughly investigated by scanning electron microscopy (SEM).

**Keywords:** Micro hardness, Debye temperature, Poisson's ratio, FT-IR spectroscopy, Scanning electron microscopy, X-ray diffractometry

### 1 Introduction

The propagation of ultrasonic wave in solids such as glass provides valuable information regarding the solid state motion in the material. Interest in glasses has rapidly increased in recent years because of diverse applications in electronic, nuclear, solar energy and acoustic optic devices. The acoustic wave propagation in bulk glasses has been of considerable interest to understand the mechanical properties<sup>1</sup>. The velocity of sound is particularly suitable for characterizing glasses as a function of composition because it gives information about the microstructure and dynamics of glasses<sup>2</sup>. The study of elastic properties of the glasses has inspired many researchers<sup>3,4</sup> and significant information about the same has been obtained. The elastic moduli of glasses are influenced by the many physical parameters, which may in turn be studied by measuring the ultrasonic velocities. The dependence of ultrasonic velocity on the composition of glass indicates the various changes in the structural configuration between the network former and modifiers<sup>5</sup>.

Glass structure is a basic issue to understand the behaviour of the material, the velocity of ultrasonic waves and hence, the elastic moduli are particularly suitable for characterizing glasses as a function of composition<sup>6</sup>. Ultrasonic investigation of solids is

gaining much importance nowadays and interest in glasses has rapidly increased because of improving information technology. Elastic properties are very informative about the structure of solids and they are directly related to inter atomic potentials. In recent years, attention has been focused more on glassy materials in few of their larger optical nonlinearity and high optical quality with fast response time<sup>7</sup>. Ultrasonic tools are very important for characterizing materials because they have many applications in physics, chemistry, food industry, medicine, oceanography, seismology, and so forth. Boron oxide is one of the best glass formers and its structure consists of a sheet-like arrangement of boron-oxygen triangles connected at all corners to form a continuous network<sup>8</sup>. Physical properties of borate glasses can often be altered by the addition of a commonly used network modifiers to the basic constituent. The commonly used network modifiers are the alkali and alkaline earth oxides.

The more interesting is that glasses containing  $Bi_2O_3$  and  $SiO_2$  have attracted a considerable attention due to their wide applications in the field of glass ceramics, thermal and mechanical sensors, reflecting windows, or may be used as layers or optical and optoelectronic devices, etc. These glasses have a long infrared (IR) cut-off and high third order nonlinear

optical susceptibility which make them ideal candidates for applications as infrared transmission components ultrafast optical switches and photonic devices<sup>9,10</sup>. It is well known that the Bi<sub>2</sub>O<sub>3</sub> is not classical glass network former. Nevertheless, glasses based on Bi<sub>2</sub>O<sub>3</sub> show interesting physical properties such as a high density, a high linear and non-linear refractive index enabling their extensive various applications in optics and optoelectronics<sup>11</sup>.

In the present paper, the ultrasonic velocity (both longitudinal and shear) and density for the two serious glass systems, (i) B<sub>2</sub>O<sub>3</sub>-SiO<sub>2</sub>-Na<sub>2</sub>CO<sub>3</sub>(BSS-glass systems) (ii) B<sub>2</sub>O<sub>3</sub>-Bi<sub>2</sub>O<sub>3</sub>-Na<sub>2</sub>CO<sub>3</sub> (BBS-glass systems) using pulse-echo technique, have been measured. The elastic constants such as longitudinal modulus (L), shear modulus (S), bulk modulus (K), young's modulus (E), Poisson's ratio ( $\sigma$ ), acoustic impedance (Z), micro hardness (H), Debye temperature ( $\theta_D$ ), and thermal expansion co-efficient ( $\alpha_p$ ), molar volume ( $V_m$ ), oxygen packing density (O), ionic concentration (N), and inter ionic distance of the prepared glass samples have been calculated, which throw more vital information about the rigidity and structure of glasses. The authors also have undertaken spectroscopic, XRD and scanning electron microscopic (SEM) study to substantiate their structural elucidation studies as presented in Tables 1-7.

**2 Experimental Details**

The chemicals used in the present research work were Analytical Reagent (AR) and Spectroscopic Reagent (SR) grade with minimum assay 99% were

obtained. The composition in mol% of B<sub>2</sub>O<sub>3</sub> is kept constant and varying of mol% of SiO<sub>2</sub> in system – I (BSS-glass systems) and mol% of Bi<sub>2</sub>O<sub>3</sub> in system – II (BBS-glass systems) glass specimen are listed in Table 1. The required amounts (approximately 20 g) in mol% of chemicals were weighed using a single pan digital balance (Model: Shimadzu, AX-200, Japan make) having an accuracy of 0.0001 g. The homogenization of the appropriate mixture of the component of chemicals was effected by repeated grinding using a pestle and mortar. The mixture is melted in platinum crucible and the temperature controlled muffle furnace was gradually raised to a higher temperature at the rate of 100 K per hour and a glassily structure was noticed for BSS glass systems

Table 1 — Composition of glass specimen

S.No.	Glass specimen	Composition in mol %	Remark
System I (B <sub>2</sub> O <sub>3</sub> - SiO <sub>2</sub> -Na <sub>2</sub> CO <sub>3</sub> )			
1	BSS-1	60-12-28	Mol% of B <sub>2</sub> O <sub>3</sub> is kept constant
2	BSS-2	60-14-26	
3	BSS-3	60-16-24	
4	BSS-4	60-18-22	
5	BSS-5	60-20-20	
6	BSS-6	60-22-18	
System II (B <sub>2</sub> O <sub>3</sub> - Bi <sub>2</sub> O <sub>3</sub> -Na <sub>2</sub> CO <sub>3</sub> )			
1	BBS-1	60-12-28	Mol% of B <sub>2</sub> O <sub>3</sub> is kept constant
2	BBS-2	60-14-26	
3	BBS-3	60-16-24	
4	BBS-4	60-18-22	
5	BBS-5	60-20-20	
6	BBS-6	60-22-18	

Table 2 — Values of density ( $\rho$ ), longitudinal velocity( $U_L$ ), shear velocity( $U_S$ ), and elastic moduli of BSS and BBS glass systems

Name of the glass samples	Ultrasonic Velocity U (m/s)			Elastic Moduli			
	Density ( $\rho$ ) Kg/m <sup>3</sup>	Longitudinal Velocity ( $U_L$ )	Shear Velocity( $U_S$ )	Longitudinal Moduli (L) $\times 10^9$ Nm <sup>-2</sup>	Shear Moduli (G) $\times 10^9$ Nm <sup>-2</sup>	Bulk Moduli (K) $\times 10^9$ Nm <sup>-2</sup>	Young's Moduli (E) $\times 10^9$ Nm <sup>-2</sup>
System I (B <sub>2</sub> O <sub>3</sub> - SiO <sub>2</sub> -Na <sub>2</sub> CO <sub>3</sub> ) BSS-glass systems							
BSS-1	1540.63	4380.61	2291.46	29.56	8.089	17.475	21.29
BSS-2	1736.49	4391.02	2388.18	33.71	9.429	18.143	24.61
BSS-3	1748.61	4498.25	2618.78	35.13	11.854	19.330	30.1
BSS-4	1765.66	5172.93	2884.59	47.24	14.591	27.65	36.59
BSS-5	1783.32	5333.33	3089.35	50.72	17.02	28.03	42.46
BSS-6	1798.72	5422.22	3096.58	52.88	17.247	29.887	43.40
System II (B <sub>2</sub> O <sub>3</sub> - Bi <sub>2</sub> O <sub>3</sub> -Na <sub>2</sub> CO <sub>3</sub> ) BBS-glass systems							
BBS-1	1350.36	4936.74	2727.37	32.98	10.06	19.564	25.28
BBS-2	1340.03	4800.00	2640.90	30.87	9.345	18.414	23.91
BBS-3	1320.36	4723.10	2620.41	29.67	9.134	17.498	23.52
BBS-4	1310.97	4646.91	2125.06	28.30	5.919	17.043	16.1
BBS-5	1294.98	4376.52	2017.45	28.40	5.270	16.521	14.38
BBS-6	1292.39	4128.67	1888.87	22.02	4.611	15.879	12.62

Table 3 — Values of Poisson's ratio ( $\sigma$ ), acoustic impedance (Z), microhardness (H), Debye temperature ( $\theta_D$ ) and thermal expansion coefficient ( $\alpha_p$ ) of BSS and BBS glass systems

Name of the glass samples	Poisson's ratio ( $\sigma$ )	Acoustic impedance Z ( $\times 10^7$ kg.m <sup>2</sup> s <sup>-1</sup> )	Micro harness H ( $\times 10^{-9}$ Nm <sup>-2</sup> )	Debye temperature ( $\theta_D$ )K	Thermal expansion co-efficient $\alpha_p$ .K <sup>-1</sup>
System I (B <sub>2</sub> O <sub>3</sub> - SiO <sub>2</sub> -Na <sub>2</sub> CO <sub>3</sub> ) BSS-glass systems					
BSS-1	0.311	0.6748	0.109	173.47	101616.82
BSS-2	0.305	0.7678	0.122	183.22	101858.42
BSS-3	0.274	0.781	0.178	204.16	104346.07
BSS-4	0.245	0.913	0.249	227.43	119998.64
BSS-5	0.247	0.951	0.246	243.60	123719.92
BSS-6	0.258	0.955	0.278	245.18	125782.17
System II (B <sub>2</sub> O <sub>3</sub> - Bi <sub>2</sub> O <sub>3</sub> -Na <sub>2</sub> CO <sub>3</sub> ) BBS-glass systems					
BBS-1	0.280	0.668	0.147	141.04	114519.03
BBS-2	0.282	0.643	0.135	136.16	111346.67
BBS-3	0.287	0.628	0.129	134.69	109562.59
BBS-4	0.367	0.609	0.052	109.97	107794.99
BBS-5	0.365	0.566	0.047	106.57	101521.93
BBS-6	0.367	0.533	0.040	103.87	95771.81

Table 4 — Values of physical parameter of the BSS and BBS glass system

Name of the sample	Average molecular weight (M) (g/mol)	Molar volume (V <sub>m</sub> ) (cm <sup>3</sup> /mol)	Oxygen packing density (O) (10 <sup>-6</sup> m <sup>3</sup> /mol)	Ionic concentration (N) (10 <sup>21</sup> /cm <sup>3</sup> )	Inter ionic distance R(A)
System – I (B <sub>2</sub> O <sub>3</sub> -SiO <sub>2</sub> -Na <sub>2</sub> CO <sub>3</sub> )					
BSS-1	78.6516	51.052	56.4124	5.6629	0.56135
BSS-2	77.7322	44.7661	60.8873	7.5344	0.51043
BSS-3	76.8128	43.9281	64.6509	8.7750	0.48517
BSS-4	75.8934	42.9828	65.6050	10.0885	0.46283
BSS-5	75.1540	42.1384	66.4476	11.434	0.44424
BSS-6	74.2526	41.2812	67.3429	12.8393	0.42742
System – II (B <sub>2</sub> O <sub>3</sub> -Bi <sub>2</sub> O <sub>3</sub> -Na <sub>2</sub> CO <sub>3</sub> )					
BBS-1	127.2644	95.7408	31.3345	2.2647	0.76149
BBS-2	134.5638	100.4201	29.8741	2.5190	0.73517
BBS-3	141.7632	107.3719	27.9402	2.6925	0.71883
BBS-4	148.9626	113.6338	26.4005	2.8621	0.70456
BBS-5	156.162	120.6443	24.8665	2.9954	0.69374
BBS-6	163.3614	126.4113	23.7320	3.1445	0.68259

Table 5 — System-I B<sub>2</sub>O<sub>3</sub>-SiO<sub>2</sub>-Na<sub>2</sub>CO<sub>3</sub> (BSS-glass system)

Glass Name	Peak's Positions(cm <sup>-1</sup> )								
	467.12	536.78	1007.67	1350.23	2359.35	2426.34	2857.43	2926.55	3773.5
BSS-1	467.12	536.78	1007.67	1350.23	2359.35	2426.34	2857.43	2926.55	3773.5
BSS-2	469.25	538.54	1009.21	1350.88	2357.95	2432.31	2859.71	2926.03	3771.43
BSS-3	465.10	523.54	1005.32	1348.87	2361.65	2438.39	2857.79	2925.65	3763.03
BSS-4	467.56	532.87	1009.34	1352.65	2357.76	2430.76	2859.90	2924.17	3771.14
BSS-5	467.87	532.81	1015.33	1364.44	2359.69	2419.11	2857.51	2924.77	3777.43
BSS-6	471.76	530.12	1026.99	-	-	2430.66	2862.05	2926.12	3794.24

at 1100 K and for BBS glass systems at 1140 K. The molten glass melt was immediately poured on a heavy copper molding block having the dimension of 12 mm diameter and 6 mm length kept at room temperature. Then the glass samples were annealed at 400 K for two hours to avoid the mechanical strains developed during the quenching process. The two opposite faces

of glass were highly polished to ensure a good parallelism. All glasses are cleaned with acetone to remove the presence of any foreign particles. The samples are prepared chemically stable and non-hygroscopic and such glass samples as System – I (BSS) and System – II (BBS) are reported in Plate-1 and Plate-2.

Table 6 — System – II B<sub>2</sub>O<sub>3</sub>-Bi<sub>2</sub>O<sub>3</sub>-Na<sub>2</sub>CO<sub>3</sub> (BBS-glass system)

Glass name	Peak's positions(cm <sup>-1</sup> )							
BBS-1	471.04	534.69	710.12	1005.35	1362.02	2924.98	3428.13	3715.63
BBS-2	471.18	534.91	700.34	1001.09	1350.55	2924.17	3435.76	3726.44
BBS-3	474.15	534.28	702.56	995.67	1350.14	2924.67	3424.16	3721.69
BBS-4	473.91	534.45	704.87	995.21	1346.89	2924.39	3420.26	3726.23
BBS-5	476.84	530.10	702.13	988.87	1348.38	2922.19	3426.53	-
BBS-6	490.29	-	708.43	989.98	1352.65	2926.78	3424.81	3701.11

Table 7 — Band assignment of BSS and BBS glass samples

Wave number cm <sup>-1</sup>	Band assignment
465.71-490.29	Si-O-Si and O-Si-O bending modes
523.24-538.54	Bi-O-Bi bending vibration modes
700.34-710.12	Assigned to the bending vibrations of B-O linkages in the borate network
995.21-1026.99	Assigned to the B-O stretching vibrations of BO <sub>4</sub> tetrahedra
1350.14-1381.34	B-O stretching vibrations of trigonal BO <sub>3</sub> units
2359.35-2926.78	OH stretching vibrations
3420.26-3437.65	Stretching vibrations of molecular water
3701.11-3794.24	B-OH

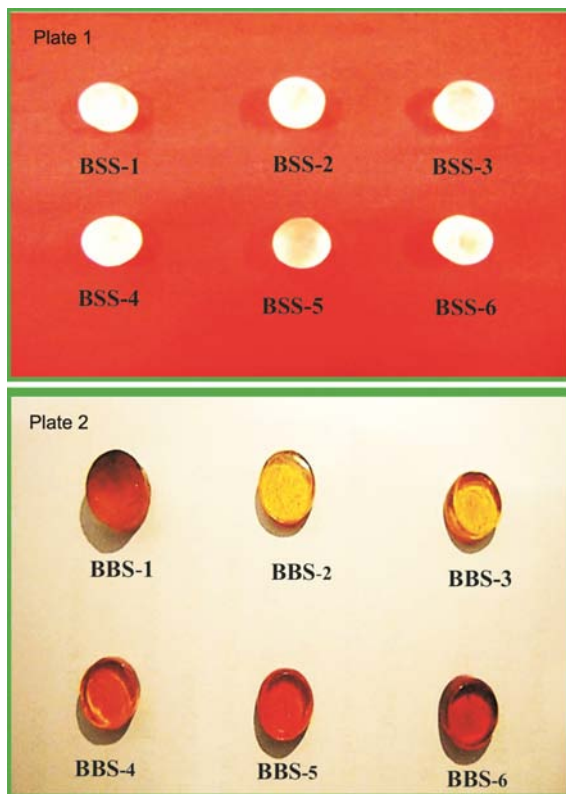


Plate — (1) BSS and (2) BBS glass systems

The ultrasonic longitudinal ( $U_L$ ) and shear velocities ( $U_S$ ) of the glass specimen were determined by using the pulse-echo method at room temperature at a frequency of 5 MHz with X-cut and Y-cut transducers. These transducers act as both transmitters and receivers of the ultrasonic pulse. The transducers

were brought into contact with each of the twelve samples by means of a couplet, in order to ensure that there was no air void between the transducer and the specimen. By applying constant pressure on the probe, the echo waveforms were obtained on the display unit and stored in the memory. Figure 1(a and b) shows one such echo waveforms obtained for longitudinal as well as for shear waves (for BSS & BBS systems).

The density of the glass samples was measured using relative measurement method. Benzene was used as a buoyant liquid. The glass samples were weighed both in air and after immersing in benzene at 303 K. The weight of the glass samples was measured in a single pan with an accuracy of 0.0001 g. The density was calculated using the formula:

$$\rho = \rho_B \frac{W_1}{W_1 - W_2}$$

where  $W_1$  and  $W_2$  are the weights of the glass samples in air and in benzene and  $\rho_B$  is the density of the benzene at 303 K.

### 3 Results and Discussion

X-ray diffraction studies were carried out on each glass samples to confirm the amorphous nature of prepared glasses. An X-ray diffractometer (PW1700: Philips Eindhoven, the New Netherlands) was used with CuK as a radiation source between 20° and 80°. The prepared glass samples were washed gently in double distilled water. The washed glass samples were dried at

room temperature, ground and then used to obtain the XRD patterns. The XRD spectrum shows number of evidence of unmelted crystalline particles confirming its amorphous nature. Such XRD spectrums of one of the BSS-I and BBS-II glass systems are shown in Fig. 2(a and b).

The values of density and ultrasonic velocity [both longitudinal ( $U_L$ ) and shear ( $U_S$ )] of the different glass specimens with respect to change in mol% of  $\text{SiO}_2$

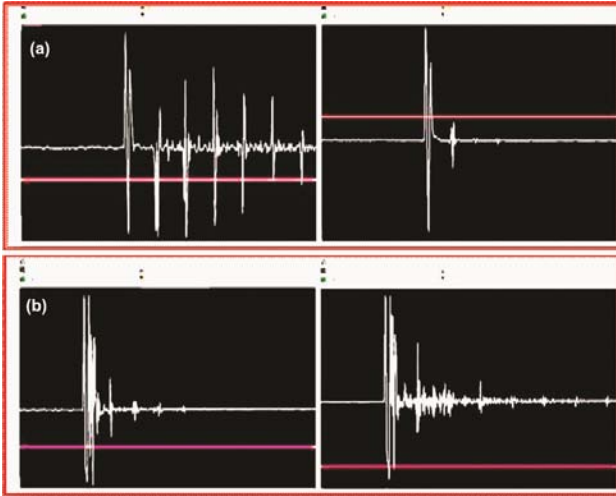


Fig. 1 — (a) Longitudinal and (b) Shear wave form for BSS & BBS-glass system

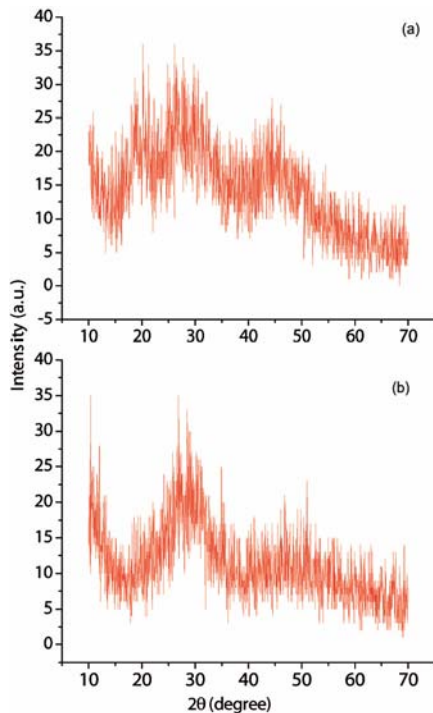


Fig. 2 — XRD pattern of (a) BSS and (b) BBS glass system

and  $\text{Bi}_2\text{O}_3$  are listed in Table 2. The calculated elastic moduli such as longitudinal modulus (L), shear modulus (G), bulk modulus (K), and young's modulus (E) are reported in Table 2. The perusal of Table 3 shows the values of Poisson's ratio ( $\sigma$ ), acoustic impedance (Z), micro hardness (H), Debye temperature ( $\theta_D$ ), and thermal expansion co-efficient ( $\alpha_p$ ) for the two glass systems (BSS and BBS). The perusal of Table 4 shows the values of oxygen packing density (O), molar volume ( $V_m$ ) and inter ionic distance  $R(A)$  for two glass systems. Fig. 4(a) shows the variation of Debye temperature for the BSS glasses with the composition of  $\text{SiO}_2$  (mol%), and Fig. 4(b) shows the variation of the same with content of  $\text{Bi}_2\text{O}_3$  in BBS-glass systems.

The density is a simple, but efficient tool capable of exploring the changes occurring in the structure of glasses. The density is affected by the structural softening or compactness, the changes in geometrical configuration, co-ordination number of ions and the dimension of interstitial space of the glass. An increasing trend in BSS-glass system with addition of  $\text{SiO}_2$  with  $\text{B}_2\text{O}_3$  is noticed and however, the second BBS-glass system shows a decreasing trend with addition of  $\text{Bi}_2\text{O}_3$  with  $\text{B}_2\text{O}_3$  content. From Table 2, one can observe a monotonic increase in BSS-glass system with content of  $\text{SiO}_2$  with  $\text{B}_2\text{O}_3$  concentration which can be attributed to the structure changes occurring in the coordination of boron glass network. The structure of crystalline as well as amorphous  $\text{B}_2\text{O}_3$  is made up of planner ( $\text{BO}_3$ ) triangle units as reported by Bray<sup>12</sup>. In amorphous  $\text{B}_2\text{O}_3$ , most of these triangles are arranged into boroxol rings in which three oxygen are outside the ring. These rings are randomly interconnected through the loose ( $\text{BO}_3$ ) units. Due to the addition of  $\text{B}_2\text{O}_3$ , the three triangle boron ( $\text{BO}_3$ ) units are converted to four coordinated boron tetrahedral ( $\text{BO}_4$ ) and thus the network dimensionality and connectivity increase. This would lead to efficient packing and compactness in the structure, which reflects an increase of density of glass systems. In the present study, the decreasing values of density in our BBS-glass systems can be attributed to the decrease in the concentration of  $\text{BiO}_6$  units upon the increase of  $\text{Bi}_2\text{O}_3$  content. A compensation of negative charge on the  $\text{BO}_4$  tetrahedron would be affected from positively charged structural defects in the  $\text{Bi}_2\text{O}_3$  sub network or from one of positive charges of  $\text{Bi}^{3+}$  cation for each  $\text{BO}_4$  tetrahedron may be the reason for decreasing of density.

The present study notices that the longitudinal ( $U_L$ ) and shear velocities ( $U_S$ ) in BSS-glass systems increase linearly with addition of mol% of  $\text{SiO}_2$  with  $\text{B}_2\text{O}_3$  content, and however, the same decrease with addition of  $\text{Bi}_2\text{O}_3$  with  $\text{B}_2\text{O}_3$  content for the BBS-glass systems are concerned. It is observed that propagation of  $U_L$  is faster than  $U_S$  in both glass systems. Bhatti and Singh<sup>13</sup> suggested that the addition of  $\text{SiO}_2$  to  $\text{B}_2\text{O}_3$  make ultrasonic velocity to increase due to change in the coordination number of boron from 3 to 4. From Table 2, the longitudinal ultrasonic velocity  $U_L$  increases from  $4380.61 \text{ ms}^{-1}$  to  $5422.2 \text{ ms}^{-1}$  for BSS glass systems and shear velocity  $U_S$  increases from  $2291.46 \text{ ms}^{-1}$  to  $3096.56 \text{ ms}^{-1}$  for BSS-glass systems. However, for the BBS glass systems, the value of  $U_L$  decreases from  $4936.74 \text{ ms}^{-1}$  to  $4128.67 \text{ ms}^{-1}$  and  $U_S$  from  $2727.37 \text{ ms}^{-1}$  to  $1888.87 \text{ ms}^{-1}$ . The decreasing trend of ultrasonic velocity in BBS-glass system can be attributed by assuming that  $\text{Ba}^{2+}$  ions enter interstitially and as a result some type of modification of B-O-B and Bi-O-B linkages which already exist in the glass may occur. Besides, the conversion of  $\text{BO}_3$  units into  $\text{BO}_4$  results in a decrease in ultrasonic velocity which affects the rigidity of the glassy nature. This behaviour indicates the replacement of  $\text{B}_2\text{O}_3$  by Bi-O-B disapproves the mechanical properties and the strength of the cross-links between chains of the borate glasses. It may also further be interpreted as the decrease of ultrasonic velocity with increasing  $\text{Bi}_2\text{O}_3$  in BBS-glass systems indicating that  $\text{Bi}_2\text{O}_3$  plays a dominant role in the velocity<sup>14</sup>. The further addition of more  $\text{Bi}_2\text{O}_3$  in glass interstices causes more ions to open up in the network leads to weakening of the glass structure or reduction in rigidity of the network. As a consequence, both velocities decrease with the addition in heavy metal oxide. Further from Higazy and Bridge<sup>15</sup>, the longitudinal strain changes directly with bond stretching force constant. Thus the increasing trend of both ultrasonic velocities may be attributed to the increase in rigidity of glass network.

Glass is considered as an elastic substance and it can be characterized through a modulus of elasticity. This modulus increase as the lengthening of certain applied stress diminishes. This will be case, if the glass structure is rigid and therefore contains the fewest possible non-bridging oxygen atoms with  $\text{B}_2\text{O}_3$  content, the structure becomes more rigid and so this leads to the increase in density as well as ultrasonic velocities<sup>16-18</sup>. So it is very obvious that an increase in

velocities is attributed to the increase in rigidity of the glass network<sup>19</sup>. Addition of  $\text{B}_2\text{O}_3$  with  $\text{SiO}_2$  increases the elastic moduli such as the longitudinal modulus (L), shear modulus (G), bulk modulus (K) and Young's modulus (E) in BSS glass system. The elevation of such elastic moduli in BSS glass system can be interpreted on the basis of the structural consideration of borate network. Further, the addition of  $\text{SiO}_2$  with  $\text{B}_2\text{O}_3$  network creates  $\text{BO}_4$  units and this leads to an increase in the network dimensionality and connectivity of the network. The increasing trend of elastic moduli in BSS-glass systems indicates resistance to deformation and is most probably due to the presence of number of layers of covalent bonds. It can be seen from Table 2, in BBS-glass systems, a decrease in elastic moduli is noticed, which is a consequence of increasing number of non-bridging oxygen atoms due to which the glass structure has further expanded.

Poisson's ratio is an effective tool in exploring the degree of cross-link density of the glass network and its magnitude increases the cross-link density, and it is the ratio of transverse and linear strains for a linear stress. According to Bridge *et.al*<sup>20</sup>, glass network having a connectivity of four (two cross-link densities) have Poisson's ratio of = 0.15. In present study, Poisson's ratio increases from 0.245 to 0.367 for both glass systems. The perusal of Table 3 exhibits the values of Poisson's ratio obtained suggesting that the network of the glasses has two-dimensional structure. The present work finds that the values of Poisson's ratio ( $\sigma$ ) found to be decreased in BSS-glass systems with addition of  $\text{SiO}_2$  with borate content, however, it finds a reverse trend with an addition of  $\text{Bi}_2\text{O}_3$  with  $\text{B}_2\text{O}_3$  in BBS-glass systems. The increase in poison's ratio with increasing content of  $\text{SiO}_2$  attributed to an increase in the average cross-link density of the glass as proposed by Higazy and Bridge<sup>15</sup>. The increasing trend of Poisson's ratio is attached to strengthening of network and hardening of the network structure. The other vital parameter micro hardness expresses the stress required to eliminate the free volume (deformation of the network) of the glass. The present study of increasing trends of micro hardness in BSS-glass systems studied [as shown in Fig 3(a)] indicates an increase in rigidity of the glass. The softening point is a temperature at which viscous flow changes to plastic flow. It determines the temperature stability of the glass. The higher value of softening temperature, the greater is the stability of its

elastic properties<sup>21</sup>. The continuous increase of micro hardness (H) in BSS-glass systems reveals the absence of non-bridging oxygen (NBO) atoms and this causes the formation of glassy network. Rajendran<sup>22</sup> observed an increase in elastic moduli and micro hardness with addition of glass former confirms the rigidity and hence there will be formation of stronger structural glassy network, which supports our investigation. Whereas, our second glass systems (BBS-systems) vary from these observation. As micro hardness values decrease [see Fig 3(b)] with increasing mol% of  $\text{Bi}_2\text{O}_3$  with  $\text{B}_2\text{O}_3$  content makes us to speculate the weakening of its compactness and rigidity of its glassy network. Hence, it is very obvious that our former type of BSS glass systems possess more compactness and rigidity over the BBS glass systems.

The Debye temperature represents the temperature at which nearly all modes of vibration in a solid are excited and its increasing trend implies an increase in rigidity of the glass. Figure 4(a and b) shows the variation of Debye temperature with  $\text{B}_2\text{O}_3$  content. The present study reveals that Debye's temperature for BSS-glass systems increases from 173.47 to 245.18K and for BBS-glass systems it decreases from 141.04 to 103.87 K over the addition of  $\text{Bi}_2\text{O}_3$  with the  $\text{B}_2\text{O}_3$  content. The gradual increase of microhardness in BSS glass systems indicates an increase in the rigidity of the glass systems. The enhancement of Debye's temperature is attributed to the increase in the number of the atoms in the chemical structure of the glass and increase in the

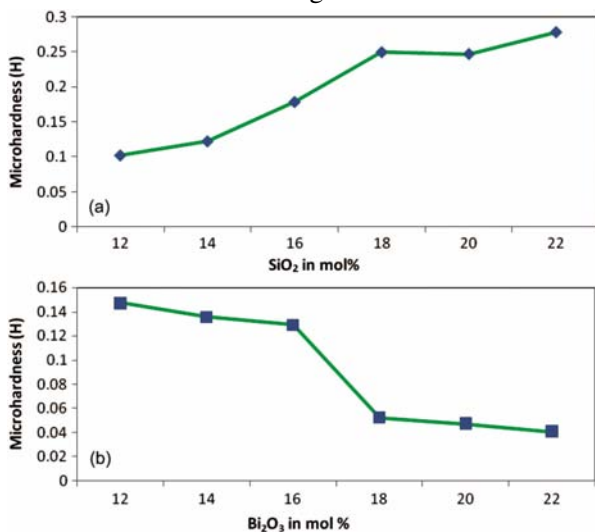


Fig. 3 — Variation of microhardness with mol % for (a) BSS and (b) BBS glass systems

ultrasonic velocity<sup>23</sup>. This elevation of Debye's temperature further stresses the strengthening in the glass structure and the higher values are reported for BSS-glass systems. The continuous increase of Debye temperature advocates the compactness in the structure leading to its rigidity.

The values of acoustic impedance (Z) are found to be increased in BSS-glass systems, whereas it exhibits a decreasing trend in BBS-glass systems. The values of acoustic impedance (Z) increase from 0.6748 to 0.9558 in BSS-glass systems, whereas, it decrease from 0.6682 to 0.5335 in BBS glass systems. The increasing of acoustic impedance has established the propagation of ultrasonic waves in the specimen and its decreasing trend has indicated the slowing down of the ultrasonic waves in the specimen. From the Table 3, it is noted that the thermal expansion coefficient ( $\theta_D$ ) increases with increasing the concentration of  $\text{SiO}_2$  in BSS-glass systems and the same decreases in BBS-glass systems with increasing concentration of  $\text{Bi}_2\text{O}_3$ . Srinivastava and Srinivasan<sup>24</sup> observed that the thermal expansion coefficient of materials depends on the strength of bonds. Therefore, the decrease in number of bonds per unit volume explains the decrease in value of thermal expansion coefficient, and hence reduction in rigidity of the glass structure in BBS-glass systems. Oxygen packing density is a measure of tightening of packing of oxide network. The present study observes that the BSS glass systems report an increasing trend of oxygen

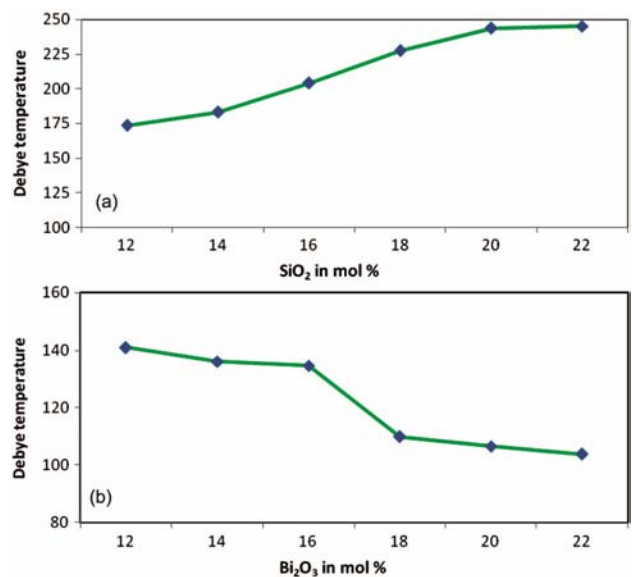


Fig. 4 — Variation of Debye temperature with mol % for (a) BSS and (b) BBS glass systems



packing density, whereas the BBS-glass systems a decreasing trend. The increasing trend of oxygen packing density in glasses reiterates that it may be tightly packed, on the other hand, the decreasing trend reveals loose packed glassy network<sup>25</sup>. The evaluated values of molar volume are reported for two glass systems in Table 4. The molar volume values are decreasing in BSS-glass systems and increasing in BBS-glass systems. The replacement of modifier  $\text{SiO}_2/\text{Bi}_2\text{O}_3$  develops more non-bridging oxygen atoms than bridging oxygen in the glass network<sup>26</sup>. The formation of non-bridging oxygen atoms may flayer-up the glass system resulting an increase of molar volume. Usually an increase in molar volume may cause a decrease in oxygen packing density, which is noticed in the present study. Table 4 also reports about the physical parameters of ionic concentration and inter ionic distance.

Structural changes after irradiation have been investigated by using FTIR spectroscopy and ultrasonic studies. According to IR analysis, there is a depolymerization of the borate network and conversion of  $\text{BO}_3$  or  $\text{BO}_4$  units with the formation of non-bridging oxygen atoms. The same study has also been employed to study the role of  $\text{Bi}_2\text{O}_3$  and  $\text{Na}_2\text{CO}_3$ , on the structure of borate glass.

$\text{B}_2\text{O}_3$  is one of the most important glass formers incorporated into various kinds of glass system as a flux material in order to attain materials having specific physical and chemical properties suitable for high technological applications. Boro atoms in borate crystals and glasses usually co-ordinate with either three or four oxygen atoms forming  $\text{BO}$  or  $\text{BO}_4$  structural units. These two fundamental units can arbitrarily be combined to form either 'Super-structural' units or different  $\text{BO}$  groups like boroxol rings, pentaborate, tetraborate and diborate groups, etc. The fraction of these structural units depends on the nature and concentration of the added modifiers. The fraction of these structural units depends on the nature and concentration of the added modifiers. The change in the structure of bismuth borate glasses after irradiation through ultrasonic, has been studied in the present paper.

The effect of divalent oxides such as  $\text{NaO}$ , and  $\text{SiO}_2$  and  $\text{Bi}_2\text{O}_3$  on the structure and properties of the thermally stable borate glass by means of IR and ultrasonic techniques, have been investigated. The infrared absorption spectra of the glasses were recorded in the wave number range  $400\text{-}4000\text{ cm}^{-1}$  for

BSS-glass system and  $400\text{-}1400\text{ cm}^{-1}$  for BBS-glass system with a resolution of  $4\text{ cm}^{-1}$  measured at room temperature by an infrared spectrophotometer using KBr pellet technique under pressure of 15 tons for few minutes. The various stretching and bending vibrations of a bond occur at certain quantized frequencies. When infrared radiation is passed through the substance, energy is absorbed and the amplitude of the vibration is increased. From the excited state, the molecule returns to the ground state by release of an extra energy by rotational, collision or translational processes. As a result, the temperature of the sample increases.

In the case of BSS-glass system, the IR spectra obtained for the studied glass samples are shown in Fig 5(a) (before and after irradiation, respectively). From Fig 5(a), the IR band of borosilicate glass, at a frequency of around  $3400\text{ cm}^{-1}$ , is due to the symmetric stretching of O-H groups and the signals at around  $1670\text{ cm}^{-1}$  are due to the deformation modes of O-H groups which are overlapped with BO stretching vibrations<sup>36</sup> and absorbed water molecules<sup>27</sup>. The band arising from the vibrations of the borosilicate network appears in the range  $1500\text{-}4000\text{ cm}^{-1}$ . The signal at around  $470\text{ cm}^{-1}$  is assigned to Si-O-Si

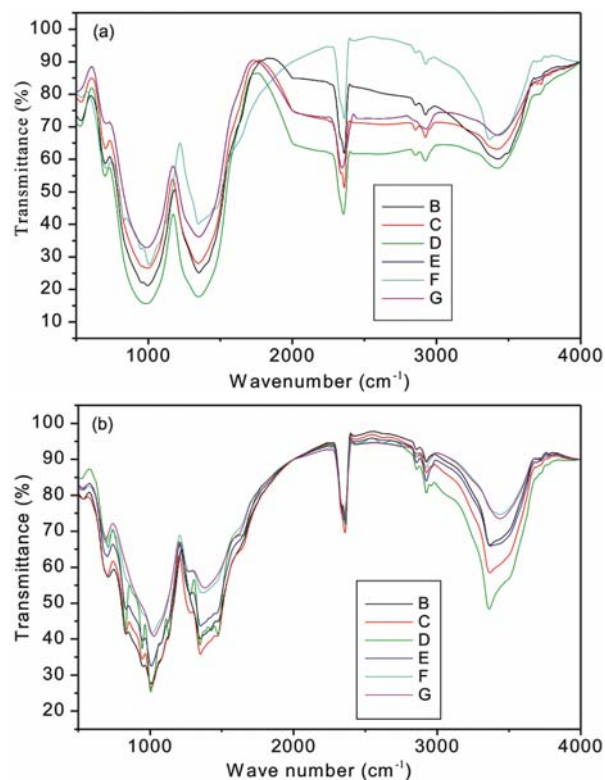


Fig. 5 — FTIR spectrum for (a) BSS and (b) BBS glass system



and O-Si-O bending modes of bridging oxygen<sup>34,35</sup> atoms overlapped with B-O-B linkages, the peak at roughly  $700\text{ cm}^{-1}$  is assigned to curve vibrations Si-O-B bridges<sup>28</sup>. The peak in the region of  $950\text{ cm}^{-1}$  is assigned to stretching vibrations of B-O bonds in BO tetrahedral. The peaks at around  $1000\text{ cm}^{-1}$  (overlapped with stretching vibration of bridging oxygen atoms (B-O) of  $\text{BO}_3$  triangles) are assigned to asymmetric stretching vibrations of NBO of  $\text{SiO}_4$  tetrahedra<sup>28</sup>. The IR analysis of the borate glasses, in general, shows four distinct frequency regions. Two regions, from  $1150$  to  $1480\text{ cm}^{-1}$  and from  $800$  to  $1150\text{ cm}^{-1}$  are assigned to the stretching vibrations of both triangular BO and tetrahedral BO borate units, respectively. Deformation modes of both types of units are active<sup>32,33</sup> between  $600$  and  $800\text{ cm}^{-1}$ . In the present work, the bands appeared at around  $1100\text{ cm}^{-1}$  are assigned to the vibration of  $\text{BO}_4$ . The band at around  $1280\text{ cm}^{-1}$  is assigned to the stretching vibrations of B-O bonds of  $\text{BO}_3$  unit involving mainly the linkage oxygen connecting different groups. By varying the chemical composition of a glass, the local environment of the transition metal ion incorporated into the network can be changed leading to inhomogeneities in the crystal field and glass work. All the FTIR spectra of the BSS glasses exhibit broad absorption bands. The lack of sharp features is indicative of the general disorder in the borate network mainly due to a wide distribution of  $\text{SiO}_2$  units occurring in this glass.

The role of  $\text{Na}_2\text{CO}_3$  in the  $\text{B}_2\text{O}_3$  network is to modify the host structure through the transformation of the structural units of the borate network form  $[\text{BO}_3]$  to  $[\text{BO}_4]$ . Sodium diborate is a type of borate glasses that consists of one-third of sodium oxide and two-thirds of boron oxide. In all systems, the  $\text{Na}_2\text{CO}_3$  is converted into  $\text{Na}_2\text{O}$  with the liberation of  $\text{CO}_2$  because of its glass transition temperature at  $1050^\circ\text{C}$ . Thus, the spectral absorption bands of  $\text{Na}_2\text{CO}_3$  are very feeble. At transition temperature, the water molecules are completely removed from the glass called 'efflorescence' or 'dehydration'. The absorption bands increase with decrease of  $\text{Na}_2\text{CO}_3$  concentration. This result is due to the modifiers (sodium oxide) which can be observed. A summary of the previous interpretation is presented Table 1 which depicts the observed IR absorption bands and their assignments.

The FTIR spectra of the glasses are considered at constant  $\text{B}_2\text{O}_3$  content and the effect of  $\text{SiO}_2$  and

$\text{Na}_2\text{CO}_3$ . In all glasses, the increase of  $\text{SiO}_2$  causes an increasing of the absorption in the range  $800$ - $1400\text{ cm}^{-1}$  corresponding to more polymerized structural units. According to IR analysis, there is a depolymerization of the borate network and conversion of  $\text{BO}_3$  or  $\text{BO}_4$  units with the formation of non-bridging oxygen atoms. Similarly in taking BBS-glass system, infrared investigations reveal structural changes and observed changes in infrared spectra due to irradiation and can be interpreted by assuming that irradiation of glass leads to formation of induced defects which lead to a decrease of the intensity of the main characteristic mid absorption bands<sup>37</sup>. Vibrational modes of borate network are mainly active in three infrared spectral regions: first region at around  $700\text{ cm}^{-1}$  is due to bending of B-O-B linkage, the second at  $900$ - $1400\text{ cm}^{-1}$  is due to B-O bond stretching of tetrahedral  $\text{BO}_4$  units and third at  $1350\text{ cm}^{-1}$  is due to stretching of trigonal  $\text{BO}_3$  units. Bismuth containing glasses have fundamental vibrations<sup>38-40</sup> in the IR spectral regions at  $700\text{ cm}^{-1}$  reveals the spectra of irradiated glasses [Fig 5(b)]. All the samples show the presence of broad band at about  $900\text{ cm}^{-1}$  and a broad band centered at  $1350\text{ cm}^{-1}$  indicates the presence of  $\text{BO}_4$  tetrahedra. The low frequency band at  $470\text{ cm}^{-1}$  is attributed totally symmetric bending vibrations of  $\text{BiO}_3$  pyramidal units. An absorption band<sup>41</sup> centered at  $534\text{ cm}^{-1}$  is observed for BBS glass composition which indicates the presence of  $\text{BiO}_6$  octahedral units and thus, octahedral provides weaker binding in the glass network in agreement with ultrasonic velocity measurements. The absorption peak around  $700\text{ cm}^{-1}$  indicates oxygen bridges between the two trigonal boron atoms.

The IR analysis of the  $\text{Bi}_2\text{O}_3$  shows a frequency region extended form  $400$ - $600\text{ cm}^{-1}$ , which is assigned to Bi-O in  $\text{BiO}_6$  octahedra<sup>42-44</sup>. The bands at around  $555$ - $590\text{ cm}^{-1}$  are the overlapping of the vibrations of the Bi-O bonds in the  $\text{BiO}_6$  octahedral unit, with the bands of the in-plane bending vibration of  $\text{BO}_3$  units<sup>45-48</sup>. Addition of  $\text{Bi}_2\text{O}_3$  will change the borate structure by creating  $\text{BO}_4$  units at the expense of  $\text{BO}_3$  structural units. The bands at  $701$ - $708\text{ cm}^{-1}$  are assigned to the bending vibrations of B-O linkages in the borate network while the bands in the region  $900$ - $1350\text{ cm}^{-1}$  are the overlapping of the vibrations of the various arrangements containing  $\text{BO}_4$  units. Accordingly, as the  $\text{Bi}_2\text{O}_3$  content increases, the intensities of the bands around  $530\text{ cm}^{-1}$  increase in intensity, and the bands of  $[\text{BO}_3]$  units are shifted to

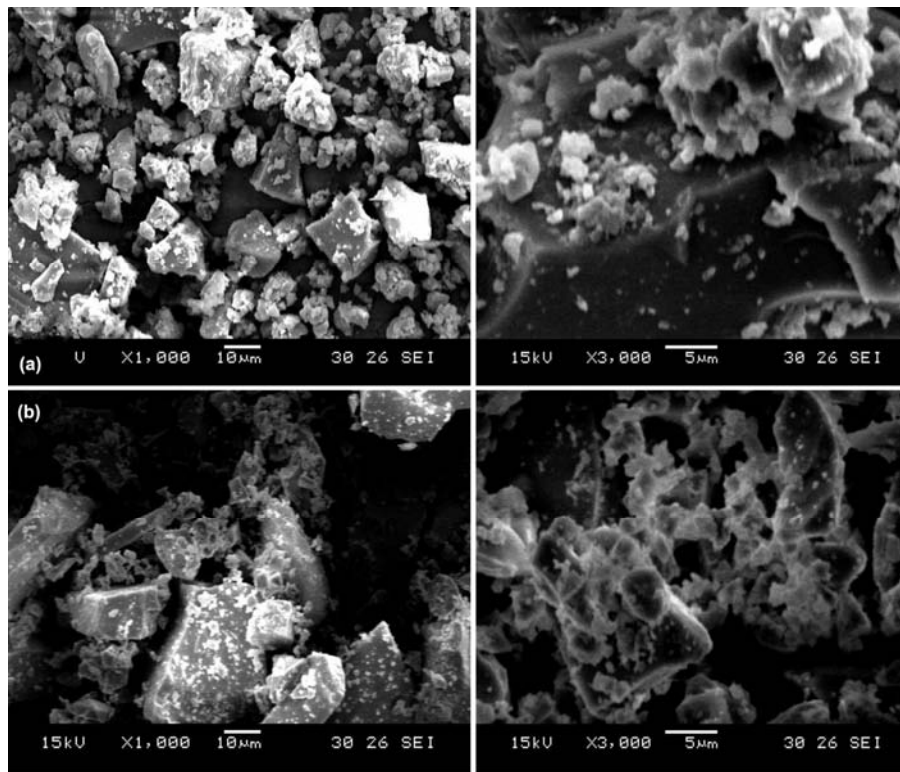


Fig. 6 — SEM micrographs of (a) BSS-glass system and (b) BBS-glass system

lower wave number. This behaviour can be explained by assuming the formation of a new bridging bond of Bi-O-B. This new bond is formed due to the inducement of the electrostatic field of the strongly polarizing  $\text{Bi}^{3+}$  ions. The infrared spectra showed that addition of  $\text{Bi}_2\text{O}_3$  causes broad absorption band arise in the region  $850\text{-}1000\text{ cm}^{-1}$ .

FTIR transmission spectra of the studied samples show vibration bands which are characteristics of triangular and tetrahedral borate units together with few small bands due to water, OH, BOH units. The FTIR spectral studies confirm the presence of various content of the title sample. An FTIR spectrum of title sample exhibits broad absorption bands indicating the wide distribution of borate structural units. The effect of  $\text{Na}_2\text{CO}_3$  and  $\text{SiO}_2$  contents on the properties and structures of BSS glass is evaluated from the FTIR spectra. The addition of  $\text{BiO}_2$  and  $\text{Na}_2\text{CO}_3$  supports the formation of borates unites with non-bridging oxygen atoms.

Scanning Electron Microscope (SEM) is used in a wide range of fields as a tool for observing surfaces at nanometer level. The main advantage of SEM is its ability to study the heterogeneity of glass composites to visualize various mineral components and their relation

in terms of overall micrographic and texture. SEM covers the observation from the fine structures on a surface of specimen to elemental analysis on a micro area without destroying the specimen.

The prepared glass samples contain well-defined randomly distributed ingrained in a glassy network. The residual glass phase is acting as interconnecting zones making the glass samples free of voids and cracks. This is also clear from scanning electron microscopy Fig. 6 (a and b).

The particles are angular or spherical in nature. The large particles may be mono mineralic, but a majority is likely to be composite (Fig. 6). Some sphere-like agglomerates were found spreading on the glass surface, due to deposition of amorphous apatite. This suggests that during glass formation, the presence of clusters composed of fibers are formed. Also, the glass may consist of large particles, aggregates, agglomerates and clusters, which clearly explain the surface of morphology of glass samples.

The SEM photographs of the samples are given in Fig. 6(a and b). It is obtained that different sized grain particles are distributed. The particle size seems to vary in each micrograph. It consists of density packed grains free from holes.

#### 4 Conclusions

The evaluated acoustical, elastic and mechanical properties of BSS and BBS glasses throw light on rigidity and compactness in structural network. The elevation of Poisson's ratio, microhardness and Debye temperature in the present study advocates the strengthening of glassy nature and hardening of the glassy network structure. From the interpretation of IR spectral analysis, the addition of  $\text{Bi}_2\text{O}_3$  and  $\text{Na}_2\text{CO}_3$  supports the formation of borate units with non-bridging oxygen atoms which was earlier confirmed in ultrasonic study. Among the two glass systems studied, the BSS glass systems possess more compactness in structural network and rigidity over the BBS glass systems.

#### References

- Pakade S V & Yawale S P, *J Pure Appl Ultrasonics*, 18 (1996) 74.
- Shree krishnakumar, Jugan J & Roshan Abraham, *J Pure Appl Ultrasonics*, 19 (1977) 32.
- Kodamma M, *Chapman & Hall Ltd*, (1991) 4048.
- Yawale S P & Pakade S V, *Acoustica*, 76 (1992)103.
- An& Pal Singh, Anita paul & Bahatti S S, *Indian J Pure & Appl Phys*, (1990) 483.
- Gaafar M S, Saddeek Y B & El-Latif L Abd, *J Phys & Chem of Solids*, 70 (2009)173.
- Nishara Begun A & Rajendran V, *Mater Lett*, 61 (2007) 2143.
- Chryssikos G D, Bitsis M S, Kapoidsis J A & Kamitsos E I, *J Non-Cryst Solids*, 217 (1997) 278.
- Venkatraman B H & Varma K B R, *Opt Mater*, 28 (2006) 1423.
- Borsa F, Torgeson D R, Martin S W & Patel H K, *Phys Rev B*, 46 (1992) 795.
- Rada S, Culea M, Pascuta P, Culea E, *J of Molecular Structure*, 937 (2009) 70.
- Bray P J & Poraikoshits E, Newyork, *Consulttant Bureau* (1996).
- Singh A P & Bahatti S S, *Indian J Pure & Appl Phys*, 483 (1990).
- Yawale S P, Pakade S V & Adgaonkar C S, *Acoustica*, 81 (1995) 184.
- Higazy A A & Bridge B, *J Non-Cryst Solids*, 72 (1985) 81.
- Saddex Y B, *Mater Chem Phys*, 83 (2004) 222.
- Saddex Y B, *Philos Mag*, 89 (2009) 41.
- Saddex Y B, *J Alloys Compd*, 467 (2009) 14.
- Saddex Y B, *Mater Chem Phys*, 91 (2005) 146.
- Bridge B, Patel N D & Waters D N, *Phys Status Solidi (a)*, 77 (1983) 655.
- Sidkey M A, Abd El-moneim & Abd El-Latif L, *Mater Chemphys*, 61 (1999) 103.
- Rajendran V R, *Proceedings of the 15<sup>th</sup> world conference on non-destructive testing 2000*.
- Sidkey M A, Moneim A & Latif L, *Mater Chem Phys*, 61 (1999) 103.
- Srivastava C M, Srinivasan C, *Science of Engineering Materials, 2nd edn, New Age International (P) Ltd*, New Delhi (1997).
- Padmaja G & Kishtaiah P, *J Phys Chem*, 113 (2009) 2397.
- Rao D S & Karat P P, *Physics & Chemistry of Glasses*, 35(3) (1994) 124.
- Hussain N S, Lopes M A & Santos J D, *Mater Chem Phys*, 88 (2004) 5.
- H&k&e M, Sitaz M, Rokita M & Galuskin E, *J Mol Struct* (2003) 651.
- Bootjomchai C, Laopaiboon J, Nontachat. S, Tipparach U & Laopaiboon R, *Nuclear Engineering & Design*, 248 (2012) 28.
- Kamitsos E, Karakassides M & Chryssikos G, *J Phys Chem*, 91 (1987) 1073.
- Kamintso E, Patsis A, Karakassides M & Chryssikos G, *J Non-Cryst Solids*, 126 (1990) 52.
- Chryssikos G, Liu L, Varsamis C & Kamitsos E, *J Non-Cryst Solids*, 235 (1998) 761.
- El-Egili K, *Physica B*, 325 (2003) 340.
- Lin S L & Hwang C S, *J Non-Cryst. Solids*, 202 (1996) 61.
- Kohly J T, Condrate R A & Shelby J E, *Phys Chem Glasses*, 34 (1993) 81.
- Yahya G, *Turk J Phys*, 27(2003)255.
- Pan A & Ghosh A, *J Non-Cryst Solids*, 271 (2000) 157.
- Karthikeyan B & Mohan S, *Physica B*, 334 (2003) 298.
- Chen G, Baccaro S, Cecilia A, Younguan Du, Mihikova E, Nikl M & Nitsch K, *Ame Ceram Soc Bull*, 80 (2001) 107.
- Hazra S & Ghosh A, *Phys Rev B*, 51 (1995) 851.
- El-Batal F H, Azooz M A & Ezz-Eldin F M, *Phys Chem Glasses*, 43 (2002) 260.
- Baia L, Stefan R, Kiefer W & Simon S, *J Raman Spectrosc*, 36 (2005) 262.
- Cheng Y, Xiao H & Guo W, *ThermochimActa*, 444 (2006) 173.
- Chowari B & RongZ, *Solid State Ionics*, 90 (1996) 151.
- Kamitsos E, Karakassides M & Chryssikos G, *J Phys Chem*, 91 (1987) 1073.
- Kamitsos E, Patsis A, Karakassides M & Chryssikos G, *J Non-Cryst Solids*, 126 (1990) 52.
- Chryssikos G, Liu L, Varsamis C & Kamitsos E, *J Non-Cryst Solids*, 235 (1998) 761.
- Yasser B, Saddeek M & Gaafar S, *Mater Chemistry & Physics*, 115 (2009) 280-286.